New Phytologist

Research

Homologs of the *STYLISH* gene family control nectary development in *Aquilegia*

Ya Min, J. Imani Bunn and Elena M. Kramer

Department of Organismic and Evolutionary Biology, Harvard University, 16 Divinity Ave, Cambridge, MA 02138, USA

Author for correspondence:
Elena M. Kramer
Tel: +1 (617) 496 3460
Email: ekramer@oeb.harvard.edu

Received: *8 June 2018*
Accepted: *17 July 2018*

New Phytologist (2018)
doi: 10.1111/nph.15406

Key words: *Aquilegia*, co-option, nectary development, style development, *STYLISH*.

Summary

- Floral nectaries are an interesting example of a convergent trait in flowering plants, and are associated with the diversification of numerous angiosperm lineages, including the adaptive radiation of the New World *Aquilegia* species. However, we know very little as to what genes contribute to nectary development and evolution, particularly in noncore eudicot taxa.
- We analyzed expression patterns and used RNAi-based methods to investigate the functions of homologs from the *STYLISH* (*STY*) family in nectar spur development in *Aquilegia coerulea*.
- We found that *AqSTY1* exhibits concentrated expression in the presumptive nectary of the growing spur tip, and triple gene silencing of the three *STY*-like genes revealed that they function in style and nectary development. Strong expression of *STY* homologs was also detected in the nectary-bearing petals of *Delphinium* and *Epimedium*.
- Our results suggest that the novel recruitment of *STY* homologs to control nectary development is likely to have occurred before the diversification of the Ranunculaceae and Berberidaceae. To date, the *STY* homologs of the Ranunculales are the only alternative loci for the control of nectary development in flowering plants, providing a critical data point in understanding the evolutionary origin and developmental basis of nectaries.

Introduction

There are numerous cases of convergent traits in flowering plants, and the presence of floral nectaries is an interesting example. Floral nectaries are secretory glands associated with floral organs, and are considered to have arisen many times independently (Brown, 1938; Bernardello, 2007). The taxonomic and evolutionary significance of floral nectaries has been acknowledged by numerous naturalists throughout the history of science, and is considered one of the most important agents facilitating the mutualistic relationship between flowering plants and animals (Heil, 2011; Erbar, 2014).

Nectaries are very simple at one level: they are always composed of secretory tissues, produce solutions that are predominantly rich in sugar, and serve a function in the attraction of pollinators and/or defenders (Pacini *et al.*, 2003). On the other hand, floral nectaries are very diverse in terms of their position, structure and secretory mechanism (Pacini *et al.*, 2003; De La Barrera & Nobel, 2004). Therefore, it is rather surprising to find that the formation of a variety of nectaries in core eudicot taxa are controlled by orthologs of the same gene, *CRABS CLAW* (*CRC*) (Bowman & Smyth, 1999; Lee, 2005; Fourquin *et al.*, 2007). *CRC* encodes a transcription factor that belongs to the YABBY family and was initially identified in *Arabidopsis thaliana* (Bowman & Smyth, 1999). *CRC* orthologs appear to perform a deeply conserved function in gynoecium development across the angiosperms, but they also control nectary development in divergent taxa from the core eudicot clade, possibly reflecting common inheritance of a nectary identity program or, alternatively, independent parallel co-option (Lee, 2005; Fourquin *et al.*, 2007). Nonetheless, aside from *CRC*, we know little about the other genes contributing to nectary development, particularly in noncore eudicot taxa. For example, in basal eudicot genus *Aquilegia* (Ranunculaceae), the expression of *AqCRC* was detected in the carpels but not in the nectaries (Lee, 2005).

The only other common theme in our understanding of nectary development and function is the involvement of auxin in nectar secretion. Since the 1950s, experiments in diverse taxa have found that exogenous application of auxin promotes the secretion of nectar in some taxa but inhibits it in others (Matile, 1956; Shuel, 1964, 1978). During *A. thaliana* flower development, a high concentration of free auxin is found in the nectaries, but the timing of this auxin response peak coincides with pollination, which is much later than the expression of *CRC* (Bowman & Smyth, 1999; Aloni *et al.*, 2006). Moreover, *PIN-FORMED6*, a member of the auxin efflux carrier family, appears to be the only gene involved in the auxin synthesis/response network that exhibits nectary-specific expression pattern in *A. thaliana*, with its expression level being positively correlated with total nectar production (Bender *et al.*, 2013).

Although we know relatively little about their genetic regulation, floral nectaries are found in many lineages outside the core eudicots and have been associated with the diversification of many clades (Neiland & Wilcock, 1998; Heil, 2011). For instance, in *Aquilegia* the elaborated petal spurs bearing nectaries in their distal tip are regarded as a textbook example of a key innovation (Whittall & Hodges, 2007) and, as such, are likely to have facilitated the recent radiation of the genus. In an effort to understand the genetic basis of nectar spur development in *Aquilegia*, a previous RNA-sequencing (RNAseq) study investigated gene expression profiles during what has been termed Phase I of petal spur development. This phase is characterized by localized cell divisions that occur in the area surrounding the nascent spur, resulting in the out-pocketing of the nectary cup from the initially laminar petal primordium (Yant *et al.*, 2015). The top differentially expressed gene when comparing the developing nectary cup (where cell division is localized) to the distal blade region (where cell division has ceased) was a gene belonging to the *STYLISH* (*STY*) family (also referred as the *SHORT INTERNODES*/*STY* family) of transcription factors (Yant *et al.*, 2015). Members of the *STY* family encode a group of plant-specific transcription factors that are required for carpel fusion and the correct development of the style and stigma in *A. thaliana* (Kuusk *et al.*, 2002, 2006; Sohlberg *et al.*, 2006; Gomariz-Fernández *et al.*, 2017). They function redundantly in a dosage-dependent manner, regulating auxin homeostasis during plant development, in large part by directly activating *YUCCA4* (*YUC4*) and *YUC8*, which encode auxin biosynthesis enzymes (Kuusk *et al.*, 2006; Sohlberg *et al.*, 2006; Eklund *et al.*, 2010a; Ståldal *et al.*, 2012). Regulatory interactions between *STY* and auxin synthesis have been found in both *A. thaliana* and the moss *Physcomitrella patens* (Eklund *et al.*, 2010b; Landberg *et al.*, 2013), suggesting deep conservation of this module across the land plants.

However, further analysis of the *Aquilegia coerulea* petal RNAseq data revealed that even though all putative *Aquilegia STY* homologs had strong spur cup-specific expression, similar enrichment patterns were not found for any homologs of the *YUC* genes or of any other known target of *A. thaliana STY1* (Yant *et al.*, 2015), raising questions regarding the role of *AqSTY* in sculpting *Aquilegia* petal spurs. Here, we conducted functional studies of the members of the *STY* family in *A. coerulea* (*AqSTY*), and revealed that the *AqSTY* genes not only execute a conserved function in carpel development, but also control nectary formation. This nectary-specific function has not been found in any previous study of *STY* homologs (Kuusk *et al.*, 2002, 2006; Eklund *et al.*, 2010b, 2011; Ståldal *et al.*, 2012; Gomariz-Fernández *et al.*, 2017). We also analyzed the expression of *STY* homologs in other taxa from the eudicot order Ranunculales, and our results indicate that *STY* genes may share a function in controlling nectary development across divergent lineages. Since the identification of *CRC* as a master regulator of nectary development in 1999, the ranunculid *STY* genes are only the second group of loci discovered to control floral nectary development.

Materials and Methods

Identification of the candidate genes

The locus identifiers of the *Aquilegia STY*-like genes were obtained from the previous RNAseq data: Aqcoe6G257900, Aqcoe5G181200 and Aqcoe2G040300 (Yant *et al.*, 2015). To confirm their orthology, a 123-locus alignment containing putative *STY*/*SHI* gene family homologs was constructed via BLAST searches in GenBank, Phytozome and the DFCI Plant Gene Index, including previously identified *STY* family members from *A. thaliana*, *Populous trichocarpa*, *Oryza sativa*, *Lycopersicon esculentus*, *Nicotiana benthaniana*, *Medicago truncatula*, *Solanum tuberosum*, *Zea mays*, *Vitis vinifera*, *Selaginella moellendorfii* and *P. patens* (Kuusk *et al.*, 2006; Eklund *et al.*, 2010b; Topp & Rasmussen, 2012). All amino acid sequences were aligned using CLUSTALW (Larkin *et al.*, 2007) as implemented in MACVECTOR (Gary, NC, USA) and then adjusted by hand. A maximum likelihood phylogenetic tree was constructed using RAXML (Randomized Axelerated Maximum Likelihood; Stamatakis *et al.*, 2008) with the default model of amino acid substitution. The resultant tree was displayed by FIGTREE (http://tree.bio.ed.ac.uk/software/figtree/) and color prepared using Adobe PHOTOSHOP CC. These analyses led to the assignment of gene names to each locus: *AqSTY1* (Aqcoe6G257900), *AqSTY2* (Aqcoe5G181200) and *AqLRP* (Aqcoe2G040300).

In situ hybridization

Fragments of *AqSTY1* (280 bp), *AqSTY2* (275 bp), *AqLRP* (374 bp) and *EgSTY1* (280 bp) from nonconserved regions of the open reading frame were PCR amplified using primers listed in Supporting Information Table S1, and cloned into the pCR™4-TOPO® vector. Both sense and anti-sense probes of each gene were alkaline hydrolyzed to an average length of 150 bp. All *in situ* hybridization steps were performed as described by Kramer (2005). Slides were incubated in 1% calcofluor white for 5 min before being visualized on the Zeiss AxioImager microscope at the Arnold Arboretum of Harvard University.

Virus-induced gene silencing

To generate single and triple virus-induced gene silencing (VIGS) constructs, the same gene fragments used for the *in situ* hybridization were amplified, digested with appropriate restriction enzymes and ligated into the TRV2 vector, together with a fragment of the *A. coerulea ANTHOCYCANIDIN SYNTHASE* (*AqANS*) gene that serves as a silencing marker. *AqSTY1* was ligated using *EcoRI* and *XbaI*; *AqSTY2*, using *SacI* and *MluI*; *AqLRP*, using *MluI* and *XhoI*; and *AqANS*, using *XhoI* and *SmaI*. The TRV2 constructs were subsequently transformed into GV3101 electrocompetent *Agrobacterium* cells. In total, 349 and 400 plants were treated with *AqSTY1-AqANS*-TRV2 and plants *AqSTY1-AqSTY2-AqLRP-AqANS*-TRV2, respectively, while 100 plants were treated with *AqANS*-TRV2. *Agrobacterium* infiltration was performed according to Gould & Kramer (2007).

Quantitative real-time polymerase chain reaction

Total RNA was extracted from only *AqANS*-silenced, wild-type (WT), and *AqSTY1-AqSTY2-AqLRP-AqANS*-silenced tissues using PureLink Plant RNA Reagent (Invitrogen), and treated with Turbo DNAse (Ambion). Subsequently, cDNA was synthesized from 1 μg RNA using Superscript II reverse transcriptase (Invitrogen) and oligo (dT) primers, and used as quantitative real-time polymerase chain reaction (qRT-PCR) template after 1 : 10 dilution. Brilliant II SYBR Green QPCR Master Mix, Low ROX (Stratagene, Cedar Creek, TX, USA/La Jolla, CA, USA), was used to carry out the qRT-PCR reactions in the Stratagene Mx3005P QPCR System. At least one of the qRT primer pairs for each gene was designed to span an intron position. *AqIPP2* (*ISOPENTYL PYROPHOSPHATE:DIMETHYLALLYL PYROPHOSPHATE ISOMERASE2*) was used for normalization as it has been previously shown to have little quantitative transcriptional variation across tissues and developmental time points (Sharma *et al.*, 2011). Primer efficiencies were evaluated using six 1 : 4 dilution series, and all showed efficiencies above 90%. At least five biological replicates for both control and VIGS-treated tissue were examined. Expression for each biological sample was assayed from three replicates per reaction plate. The variability resulting from technical replicates was negligible compared with the variability from biological replicates, so only biological variability is presented here. Relative gene expression levels were calculated using the $2^{-\Delta\Delta C}{}_T$ method described in Livak & Schmittgen (2001), taking into consideration the specific primer efficiencies as well as the exact fragment lengths.

Isolation of *STY* family genes in other Ranunculales taxa

Total RNA and organ-specific RNA from nine Ranunculid taxa (*Xanthorhiza simplicissima*, *Cimcifuga racemosa*, *Delphinium exaltatum*, *Helleborus orientalis*, *Trollius laxus*, *Cocculus trilobus*, *Menispermum dauricum*, *Epimedium grandiflorum*, and *Berberis gilgiana*; Rasmussen *et al.*, 2009) were used to synthesize first strand cDNA using SuperScript II reverse transcriptase (Invitrogen, Carlsbad, CA, USA). Forward (dSTY-F1 and dSTY-F2) and reverse (dSTY-R) degenerate primers were designed based on conserved amino acid domains that were recognized via multiple alignment of the amino acid sequences of *STY* homologs in *A. coerulea*, *Nigella damascena* (provided by R. Zhang & H.Z. Kong) and *V. vinifera* (Fig. S6). The PCR products amplified using dSTY-F1 and dSTY-R were purified and used as the templates for subsequent nested PCR with dSTY-F2 and dSTY-R primers. These nested PCR products were then cloned into the pCR™4-TOPO® vector for sequencing. Predicted protein sequences were aligned and used for phylogenetic analysis as described above. Identified sequences were deposited in GenBank under MH638630-MH638642.

Locus-specific semi-qRT-PCR was conducted on cDNA prepared from dissected floral organs of *D. exaltatum* as described in Rasmussen *et al.* (2009); 30 cycles were used. Primer sequences are shown in Table S1.

Scanning electron microscopy and histology

Tissues of interest were fixed in FAA (50% ethanol, 4% formalin and 5% glacial acetic acid) and stored at 4°C. For scanning electron microscopy (SEM), samples were dehydrated through a graded ethanol series to 100% EtOH at 4°C and critical point-dried before imaging. Samples for histology were dehydrated through the same graded ethanol series, incubated in 100% Citrasolv, and embedded in Paraplast Plus (Oxford Labware, St Louis, MO, USA). Tissues were sectioned to 8 μm using a rotary microtome and stained with 0.01% Safranin O and 50% Fast Green according to the protocol described in Ruzin (1999). Images for SEM and histology were taken using a Jeol JSM-6010 LC Scanning Electron Microscope and a Zeiss AxioImager microscope, respectively, at the Arnold Arboretum of Harvard University.

Measurement of relative nectar volume in wild-type *Aquilegia coerulea* flowers

Nectar of *A. coerulea* flowers can be easily visualized under white light, and the amount of nectar was measured based on the fraction of the spur that contained nectar. The nectar amount was determined in five terminal flowers (25 petals in total) and five lateral flowers (23 petals in total) from five different individuals, measured every day at 10:00 h, 14:00 h and 18:00 h for 2 wk, during which all flowers progressed from no nectar production to abscission of the petals. The first day of nectar production was regarded as Day 1 for standardization.

Auxin application

For local treatment of petals, indole-3-acetic acid (IAA; Alfa Aesar, Tewksbury, MA, USA) was dissolved in liquid lanolin (40°C) to reach a final concentration of either 10 mM or 100 mM (the former concentration being recommended by Stieger *et al.* (2002); and the latter by Marcos & Berleth (2009)), allowed to cool to room temperature, and the paste applied to the inside of the cavity of young petal spurs using a surgical needle. Pure lanolin paste was used as a control and similarly applied. The control and 10 mM pastes were applied to eight flowers from eight different individuals, while 100 mM paste was applied to 15 flowers from 15 individuals. For each flower, two–three sepals were removed for the convenience of application, and two–three petals, adjacent to the removed sepals, were treated with IAA or pure lanolin.

Results

Identification of *STY* homologs in *Aquilegia coerulea*

The three putative *STY* homologs in *A. coerulea*, *Aqcoe2G040300*, *Aqcoe6G257900* and *Aqcoe5G181200*, were identified from the previous RNAseq analysis (Yant *et al.*, 2015). These genes encode transcription factors with two RING-like zinc finger domains and a IGGH motif, which have been previously

identified as unique features of the STY family (Eklund *et al.*, 2010a). We subsequently conducted a BLAST search of putative *STY* homologs in 24 land plant taxa and constructed a maximum-likelihood phylogenetic tree using the resultant 123 amino acid sequences (Fig. S1) in order to assign correct orthology of the *Aquilegia* loci. *Aqcoe2G040300* falls into the *LATERAL ROOT PROMORDIUM* (*LRP*) clade with strong support and is, therefore, referred to as *AqLRP*. *Aqcoe6G257900* and *Aqcoe5G181200* are both included in a well-supported clade containing *STY* homologs from the eudicots, and are named *AqSTY1* and *AqSTY2*, respectively (although these are not strictly orthologous to the *STY1* and *STY2* genes in *A. thaliana*). *AqSTY1* is of particular interest because it was the top most significantly differentially expressed gene between cup and blade samples in early developing petal spurs (Yant *et al.*, 2015).

During early stages of *A. coerulea* flower development (Table S2), all three genes (collectively termed the *AqSTY* genes) exhibit identical expression patterns in most organs (Figures 1a–f, S2a–j), including moderate expression in axillary inflorescence meristems (Figs 1a, S2f) and emerging floral primordia (Figs 1a, b, S2a,b,f,g), as well as strong expression in carpel tips (Figs 1c,d, f, S2c,d,h,i), ovule primordia and ovules (Figs 1d,e, S2e,j). However, their expression in petals diverges as development progresses (Fig. 1g–k). At stage 8, before the stamen primordia become stalked, the expression of all three *AqSTY* genes is still overlapping and concentrated at the distal tips of carpels and petals (Figs 1f, S2c,h). During stage 9, the expression of *AqSTY1* becomes diffuse throughout the young petal (Fig. 1g), but the signals of *AqSTY2* and *AqLRP* remain concentrated in the distal tip of the petal (Figs 1h, S2d,i). When the nascent petal spurs begin to emerge during stage 10, *AqLRP* is not detectable in the petal (Fig. 1k), *AqSTY2* shows diffuse expression in the growing spur cup (Fig. 1j), but *AqSTY1* exhibits concentrated expression in a restricted area of the inner surface of the growing spur tip (Fig. 1i), which approximately corresponds to the region where nectar secretory tissues develop (Antoń & Kamińska, 2015). Expression levels of three genes during later stages of *A. coerulea* flower development were also examined via qRT-PCR (Fig. S3). All three genes showed high expression levels in the young sepals, petals, stamens and carpels of stage 11B flowers, but the expression decreases in sepals, petals and carpels of blooming flowers (Fig. S3).

AqSTY homologs control style and nectary development in *Aquilegia coerulea*

In order to investigate the functions of *STY* homologs during *A. coerulea* floral development, we performed VIGS to knock down the expression of our genes of interest. All the TRV2 constructs contained a fragment of the gene *ANTHOCYANIN SYNTHASE* (*AqANS*) as a silencing marker. Because *AqSTY1* exhibited the strongest differential expression between the petal

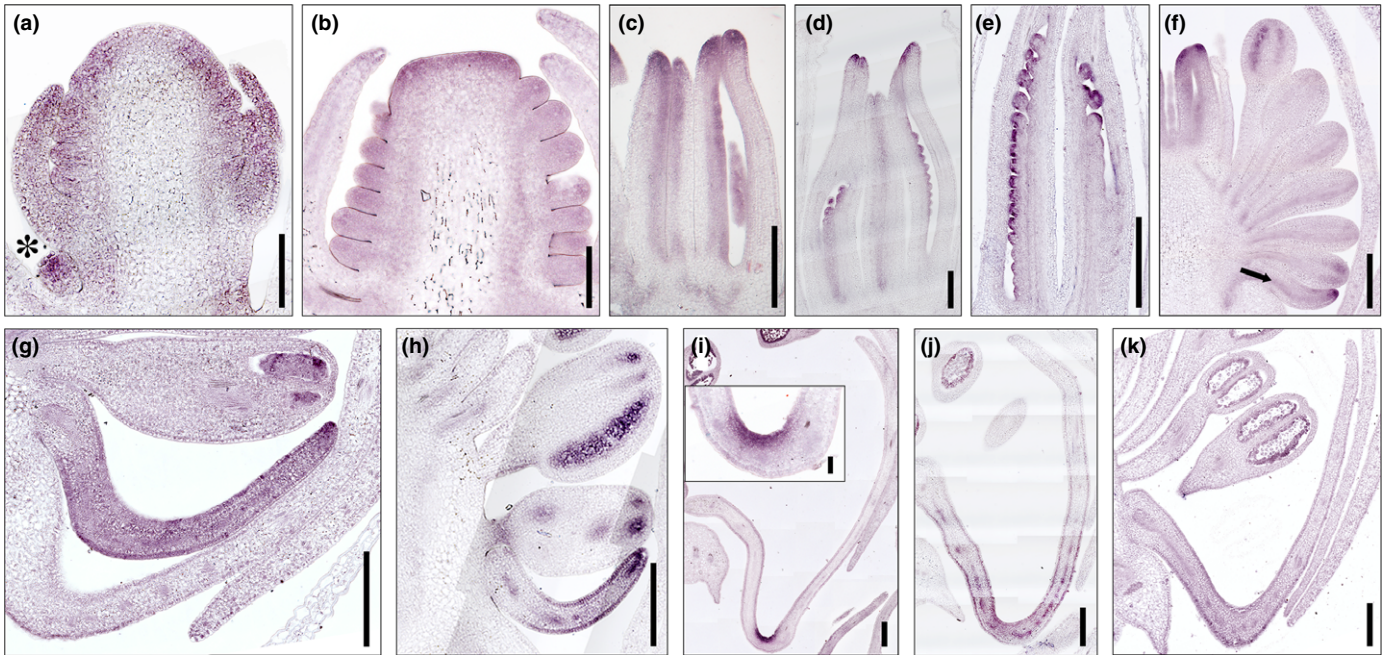

Fig. 1 Expression patterns of three *Aquilegia STY* homologs during *Aquilegia coerulea* flower development. (a–f) Expression of *AqSTY1* through various stages of flower development. *AqSTY2* and *AqLRP* show identical expression patterns in the displayed organs and developmental stages (see also Supporting Information Fig. S2). (a) Axillary inflorescence meristem (asterisk) and a stage 6 flower before the carpel primordia arise. (b) A stage 7 flower with initiating carpel primordia. (c) Stage 8 gynoecium. (d) Stage 10 gynoecium with ovules starting to initiate. (e) Close-up of initiating ovule primordia in stage 10 gynoecium. (f) All three genes showed identical expression patterns in the carpel tips and distal tips of developing petals (arrow) of a stage 8 flower (see also Fig. S2). (g–k) Petals of developmental stages during which expression of *AqSTY1*, *AqSTY2* and *AqLRP* varies. (g) Expression of *AqSTY1* in stage 9 petals when petal spurs are just starting to develop. (h) Expression pattern of *AqSTY2*, which is identical to that of *AqLRP*, in stage 9 petals. (i) Expression of *AqSTY1* in late stage 10 petal spur. Insert: close up of the expression domain of *AqSTY1* in the tip of the petal spur. (j) Expression of *AqSTY2* in late stage 10 petal spur. (k) Expression of *AqLRP* in late stage 10 petal spur is not clearly detectable. Bars: (a, b, i inset) 100 μm; (c–k) 200 μm.

blade and spur (Yant *et al.*, 2015), we first silenced the expression of *AqSTY1* alone in 349 *A. coerulea* individuals. Although 105 plants showed silencing of the *AqANS* marker and were confirmed to have specific downregulation of *AqSTY1*, no obvious morphological phenotype was recovered (Figs 3e, S4a).

Given that all three *STY* homologs were detected as cup-enriched in the previous RNAseq experiment, we prepared a TRV2 construct containing fragments of the nonconserved regions of the three genes to achieve a triple gene knock-down. Silencing of three loci plus the marker *AqANS* is expected to have a lower penetrance than targeting one or two genes, but we have had success with a multi-gene targeting approach (Sharma & Kramer, 2012). The triple-*STY* treatment resulted in no significant phenotypic change in the vegetative organs, but revealed two major floral phenotypes. First, we observed defects in stigmatic tissues and styles. In WT *A. coerulea*, the stigma becomes receptive at stage 13C, during which anther dehiscence occurs and the ventral slit of the carpel opens (Table S2). The receptive stigma can be easily observed with the naked eye as the papillae swell on the stigmatic surface. The turgid papillae cells begin to collapse by the end of stage 13D, the ventral slit will then close, and the stigma becomes dry and turns dark-yellow or brown (Fig. 2a–c; Table S2). In 40 individuals out of our 400 triple *STY*-treated flowers, however, at stage 14 and later, it appeared that the region of exposed papillae was basipetally expanded (Fig. 2d,e; Table S2). Closer examination of these styles using SEM revealed that, although the stigmatic papillae appeared normal at the cellular level, the distal portion of the ventral slit of the style remained open through development (Fig. 2f,g). Particularly, the apical portion of the style appeared to be flat, unfolded and unusually curly, rather than fused and tapering (Fig. 2d–f). qRT-PCR of these carpels confirmed that this phenotype was associated with decreased expression levels of the three *AqSTY* genes in the carpels (Fig. S4b).

Moreover, we observed that targeting all three *AqSTY* genes specifically disrupts nectary development in a subset of the silenced flowers that showed the carpel phenotype, with 12 of these flowers showing a complete loss of nectar production in multiple or all petals. *Aquilegia* nectaries are composed of several layers of nectariferous parenchyma cells that are located exclusively at the distal spur tip (Antoń & Kamińska, 2015). Each petal produces a large amount of nectar, which fills up the spur cavity and can be easily observed under light (Fig. 3a,b). Nectar is released through the rupture of epidermal cell walls, leaving a residue of the secreted material on the inner epidermal surface of the spur (Fig. 3j,m–o). WT *A. coerulea* flowers start to produce nectar at stage 12 before the sepals reflex and nectar production proceeds throughout stage 13 until the petals abscise (Table S2). This process takes *c.* 6 d, during which reabsorption of unconsumed nectar is not observed (Fig. S5). Although *AqSTY1* single knock-down flowers did not show any difference in the amount of nectar being produced (Fig. 3e,f), no nectar was observed in petals of 12 flowers, which also exhibited carpel phenotypes (Fig. 3c,d,g,h). No secretory residue was found attached to the inner epidermal wall of silenced spur tips (Fig. 3l with inset), suggesting that nectar production never occurred in these petals. In another three of the 40 triple-silenced flowers, nectar production was reduced by 50–80%, but no obvious morphological defect was observed in the nectaries.

The spur tips of the 12 nectar-deficient petals had highly variable morphologies compared with WT, and SEM and histology revealed malformation of the nectary region (Fig. 3h,l,p,q). In some cases, the parenchyma cells of the spur tips were disorganized with distorted shapes, which was associated with bulges on both outer (Fig. 3d,h,k) and inner (Fig. 3l,p) surfaces of the spur. In other nectar-deficient flowers, the parenchymal and the epidermal cells of the spur tips appeared to be very compact (Fig. 3g,q), possibly due to a lack of proper expansion and differentiation. Across all of these flowers, we did not observe a difference in petal spur lengths between the silenced and VIGS control or WT flowers, which average 5.7 cm (SD = 0.23 cm).

It should be noted that all three *AqSTY* loci are only weakly expressed in mature petals (Fig. S3), making it difficult to quantify the degree of silencing in these organs. Silencing of the three loci was clearly detected in the carpels, but expression of *AqLRP* is particularly weak in all late stage organs, which confounds our

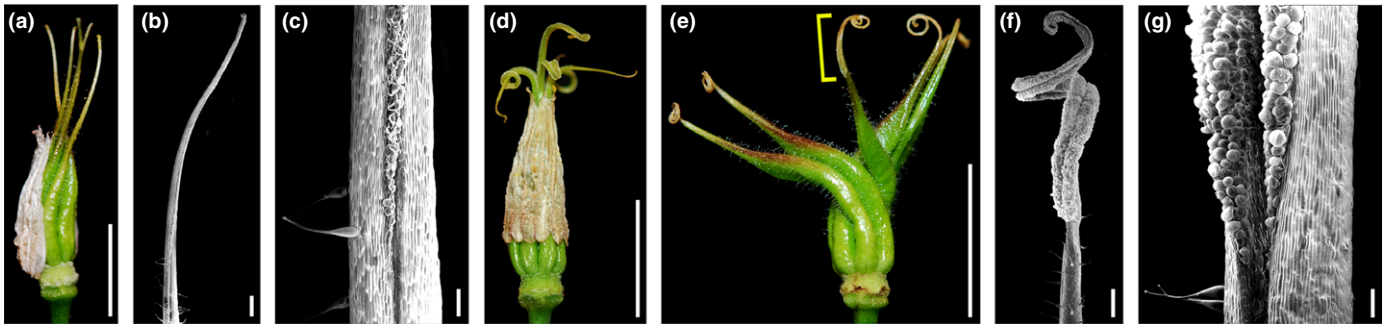

Fig. 2 Silencing of *AqSTY* genes results in defects in stylar and stigmatic tissues of *Aquilegia coerulea*. (a–c) Style and stigma morphology in wild-type (WT) *A. coerulea* gynoecium at stage 15. (b, c) Scanning electron microscopy (SEM) showing the distal portion of (b) a WT style and (c) a fused ventral slit at stage 15. (d–g) Style and stigma morphology in triple *STY*-silenced flowers. (d) Triple *STY*-silenced stage 14B gynoecium with staminodes still attached. Curly and flattened styles are very prominent. (e) Stage 15 triple *AqSTY*-silenced gynoecium. Staminodes have fallen off, styles are highly twisted (indicated by the bracket) and brown coloration is already starting to develop. (f, g) SEM showing details of distal portion of (f) a style and (g) the unfused ventral slit. Bars: (a, d, e) 1 cm; (b, f) 500 μm; (c, g) 200 μm.

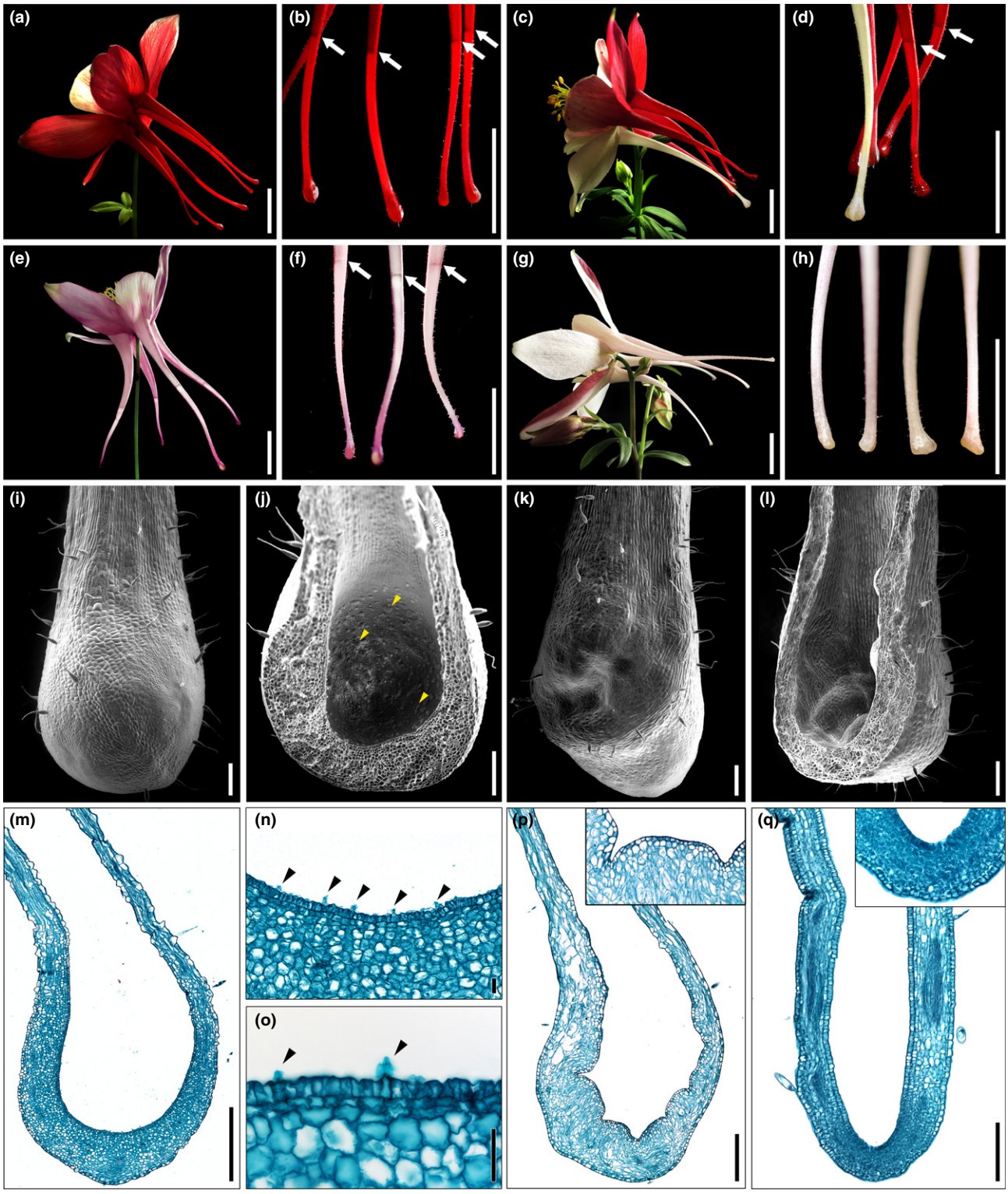

Fig. 3 Silencing of all *Aquilegia STY* homologs leads to disruption of nectary development. (a, b) A mature wild-type (WT) *Aquilegia coerulea* flower with nectar filling the petal spurs (arrows in b). (c, d) A partially triple *AqSTY*-silenced flower. Nectar fills up the red, unsilenced petal spurs (arrows in d), but no nectar is observed in the white, silenced petal spur. (e, f) A mature *AqSTY1*-VIGS flower with no change in nectar production in the petal spurs (arrows in f). (g, h) Triple *STY*-silenced flowers with distorted nectaries at the distal tips of the petal spurs that are completely lacking nectar. (i, j) Scanning electron microscopy (SEM) of the inner and outer surfaces of a WT *A. coerulea* nectary. Inset in (j) shows magnified inner surface of the nectary with residual nectar (also arrowheads in j). (k, l) SEM of the inner and outer surfaces of a triple *AqSTY*-silenced nectary. Inset in (l) shows magnified inner surface of the spur tip with no evidence of secretion. (m–o) Histology of a WT *A. coerulea* nectary, with close-ups (n, o) of nectar secretory tissue and nectar residue on the inner surfaces (arrowheads). (p, q) Histology of triple *AqSTY*-silenced nectaries, showing distortion in cellular organization (inserts). Bars: (a–h) 1 cm; (i–m, p, q) 200 μm; (n, o) 20 μm; (insets in j, l) 100 μm.

ability to demonstrate its downregulation in petals. However, these nectary-defective petals always co-occurred in flowers with affected carpels, in which we did detect silencing of all three loci.

Auxin application alone is not sufficient to induce nectary development

Because auxin biosynthesis is genetically downstream from *STY* function in highly divergent land plant taxa (Eklund *et al.*, 2010b, 2011; Baylis *et al.*, 2013; Landberg *et al.*, 2013), we examined whether nectary development could be promoted by application of exogenous IAA to the cavity (adaxial surface) of stage 11B young petal spurs (Fig. 4; Table S2). At maturity, petals treated with either 10 mM or 100 mM IAA in lanolin exhibited similar laminar distortions but no evidence of ectopic nectary development. Lanolin applied as a control did not reveal any prominent morphological change in the spurs, even when some petals were slightly damaged during the application (as in the 100 mM-treated spur shown in Fig. 4h). Cross-sections of the spurs treated with lanolin alone reveal tightly connected epidermal cells that form the inner/adaxial and outer/abaxial epidermis of the spur, and well-organized mesophyll cells surrounding each vascular bundle (Fig. 4b). IAA application in either concentration resulted in shorter but broader spur cavities with uneven and twisted laminae (Fig. 4d,f,h); however, we did not observe significant changes in the vascular patterning and histological analysis revealed that the dramatic distortions were the result of over- and/or uncoordinated proliferation of lamina tissue (Fig. 4). Although we observed some bulges on the spur surfaces (Fig. 4e,g), no evidence of nectariferous tissue formation was observed (compare Fig. 4f with Fig. 3m).

Nectary-specific expression of *STY* homologs is conserved in divergent ranunculid genera

Because previous studies of *STY* homologs in the core-eudicots and the monocots have never shown any potential role in nectar production, we were curious as to whether this role applies only to *Aquilegia*, or is conserved across the commonly nectariferous petals of the Ranunculaceae and related families. Therefore, we designed degenerate primers (Fig. S6) to amplify *STY* homologs from nine other taxa of the Ranunculales (sequences of *STY* orthologs in *N. damascena* were provided by R. Zhang and H. Z. Kong), with a particular focus on homologs of *AqSTY1* because of its nectary specific expression pattern in *Aquilegia*. The resultant predicted protein sequences were used to construct a maximum-likelihood phylogenetic tree, which was generally congruent with the phylogenetic relationships among the sampled taxa (Wang *et al.*, 2009; Fig. S7). Based on this current sampling, it appears that the duplication event that gave rise to *AqSTY1* and *AqSTY2* homologs occurred before the divergence between Ranunculaceae and Berberidaceae (Fig. S7).

We performed semi-qRT-PCR using organ-specific cDNA from *D. exaltatum* (Ranunculaceae) flowers to evaluate the expression level of the *AqSTY1* ortholog (*DeSTY1*). In addition to the strong canonical expression of *STY* homologs in carpels, high *DeSTY1* expression is detected in petals, which are associated with nectaries and have independently evolved spurs (Endress, 1995; Fig. S7). Moreover, we performed *in situ* hybridization of *EgSTY1* in young flower buds of *E. grandiflorum* (Berberidaceae). Similar to the expression pattern of *AqSTY1*, strong *EgSTY1* signal was detected in the apical portion of carpels, young ovules and nectaries of the developing petal spur

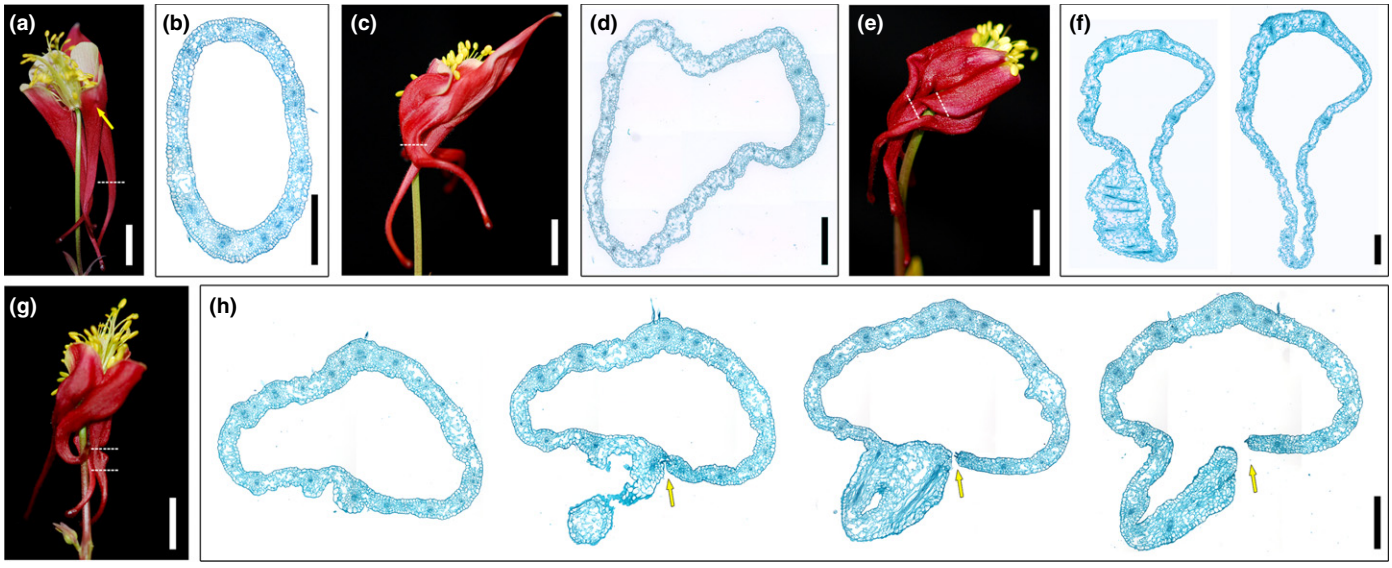

Fig. 4 Exogenous auxin application leads to distortion in petal spur formation but no ectopic nectaries. (a, b) Lanolin-treated control flower with four sepals and one petal removed (a), and a cross-section of the petal spur (b). (c, d) Ten micromolar indole-3-acetic acid (IAA)-treated flower with several sepals and one petal removed (c), and a cross-section of the petal spur (d). (e–h) Two separate 100 mM IAA-treated flowers (e, g). (f) Cross-sections of 100 mM IAA-treated petal spur of the flower shown in (e). (h) Cross-sections of 100 mM IAA-treated petal spur of the flower shown in (g). Dashed lines in (a), (c), (e) and (g) show the approximate locations of sections shown in (b), (d), (f) and (h), respectively. Yellow arrows in (h) indicate examples of needle damage during application. Bars: (a, c, e, g) 1 cm; (b, d, f, h) 500 μm.

cups (Fig. 5). These data indicate that the expression of *STY1* homologs is closely associated with nectaries in the divergent members of both the Ranunculaceae and Berberidaceae.

Discussion

Conserved functions of *STY* homologs in *Aquilegia*

Several lines of evidence provide strong support for the functional conservation of *STY* family members as regulators of auxin homeostasis across deeply divergent land plants (Sohlberg *et al.*, 2006; Eklund *et al.*, 2010b; Ståldal *et al.*, 2012; Baylis *et al.*, 2013; Landberg *et al.*, 2013); while in angiosperms, it appears that this auxin-related function is especially important for the differentiation of the distal portion of the carpels (Kuusk *et al.*, 2002; Baylis *et al.*, 2013; Gomariz-Fernández *et al.*, 2017). During early stages of *A. coerulea* flower development, the expression patterns of the *STY* homologs in floral organ primordia are consistent with that shown in other taxa, being concentrated in the distal tips of the floral organs, particularly carpels (Fig. 1). While silencing of *AqSTY1* alone did not exhibit any apparent phenotype, silencing of all three *AqSTY* homologs revealed strong defects in the styles, which become unfused and flattened, exposing large numbers of stigmatic cells (Fig. 2). Although there are differences in the details of the loss-of-function carpel phenotypes between *A. thaliana* and *A. coerulea*, it should be noted that the carpel structures in these two systems are also quite different (a syncarpous operculate capsule for *Arabidopsis* vs apocarpous dehiscent follicles for *Aquilegia*), and it is unclear exactly how auxin may contribute to carpel development in *Aquilegia*. Our current understanding of the regulation of *STY* genes focuses on a gene-family-specific GGCGGC element, which was found upstream of almost all *STY* homologs across angiosperms, either in the promoter (e.g. *AtSTY1*, *AtSTY2*, *AtSRS3*) or the 5′-UTR (e.g. *AtSHI*, *AtSRS4*, *AtSRS6*; Eklund *et al.*, 2011). Mutation of this GGCGGC element in *A. thaliana* eliminates expression in almost all shoots and distal tips of lateral organs (Eklund *et al.*, 2011). We used the sequenced *A. coerulea* genome (Filiault *et al.*, 2018) to scan 5-kb regions upstream of the start codons for each *AqSTY* locus, and similarly found the GGCGGC element in each 5′-UTR. Overall, we believe the current dataset is in line with all previous studies, which suggest deep conservation of *STY* family functions in auxin homeostasis and sculpting the apical region of angiosperm carpels. However, the triple *AqSTY*-silencing phenotype appears to be less severe than those observed in higher order combinatorial mutants of the *A. thaliana SHI* family (Kuusk *et al.*, 2006). Further study will be required to determine whether the *Aquilegia* loci play roles in vegetative development and the exact relative contributions of each homolog to these functions.

Control of floral nectary development by *Aquilegia STY* homologs is derived and may be auxin-independent

Despite their conserved function in auxin homeostasis and carpel development, we have a number of reasons to propose that the role of the *Aquilegia STY* homologs in controlling floral nectary development is recently evolved and possibly not auxin-dependent. First, the expression domain of the *Aquilegia STY* homologs in developing petal spurs is novel (Fig. 1). In contrast to the typical *STY* gene expression in the distal tips of growing organs, expression of *AqSTY1* during floral stage 8 deviates and displays moderate, diffuse expression throughout the petal. More dramatically, when the nascent petal spur starts to emerge during stage 10, *AqSTY1* is specifically expressed in the presumptive nectary, which is positioned along the midline of the organ much closer to the base than the distal tip. At the same time, unlike the *STY* genes of *A. thaliana* that are associated with auxin concentration peaks (Sohlberg *et al.*, 2006; Ståldal *et al.*, 2012; Baylis *et al.*, 2013), application of IAA to the inner surface of young petal spurs yielded malformed petal spurs but no induction of nectary-like tissue (Fig. 4). This result indicates that either auxin alone is not sufficient to induce nectary development, which could be due to multiple factors including the timing, position or concentration of the application, or that the determination of nectary identity by the *Aquilegia STY* homologs does not occur via the promotion of auxin synthesis. As mentioned above, studies in many different angiosperm systems have suggested that auxin is more likely to play a role in nectar production and secretion

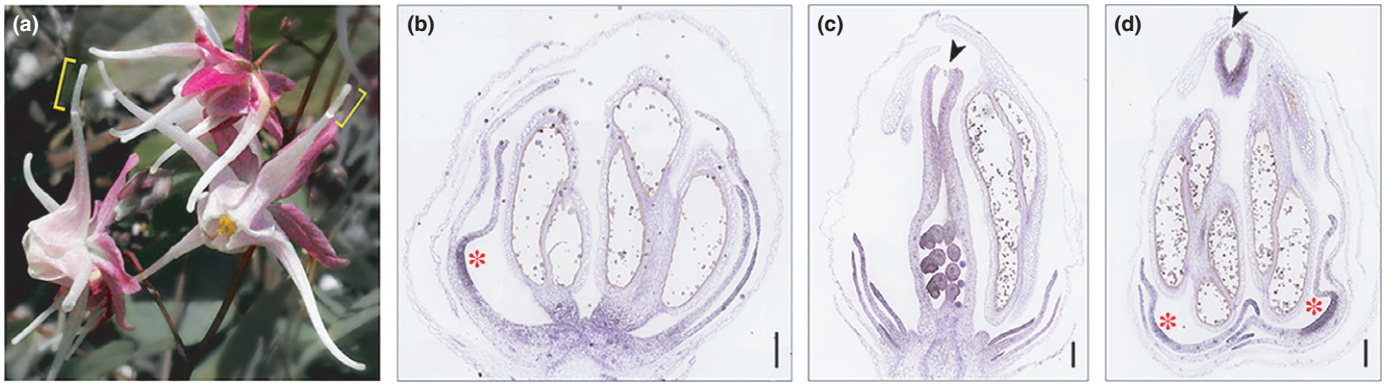

Fig. 5 Expression of *EgSTY1* in *Epimedium grandiflorum*. (a) *Epimedium grandiflorum* flowers with prominent petal spurs with nectaries located at the distal tips producing large amounts of nectar (brackets). (b–d) *In situ* hybridization of *EgSTY1* in *E. grandiflorum* flower buds. Strong signals were detected in the presumptive nectaries of the initiating petal spurs (b, d; asterisks), ovules (c) and distal tips of carpels (c, d; arrowheads). Bars, 200 μm.

rather than in determining the identity of the nectaries themselves. Perhaps most significantly, our previous RNAseq results found that while *STY* homologs all show strong spur cup-specific enrichment, no homologs of *YUC*, or any other known *STY1* target (Ståldal *et al.*, 2012), were recovered as cup-enriched (Yant *et al.*, 2015). This suggests that the otherwise conserved *STY*/auxin regulatory pathway may not apply to the nectary, but it still remains possible that some other component of canonical *STY1* function, perhaps related to cell type differentiation, has a parallel in nectary development.

The novel function of *STY* genes in nectary development was likely co-opted before the last common ancestor of the Ranunculaceae and Berberidaceae

Our expression analyses of *AqSTY1* homologs in three divergent ranunculid taxa revealed strong expression of *AqSTY1* orthologs in petals, which are broadly associated with floral nectaries in the Ranunculales (Erbar, 2014). Semi-qRT-PCR of *DsSTY1* revealed strong expression in carpels as well as petals, which are the nectar-associated organs (Fig. S7). Particularly, *in situ* hybridization of the *AqSTY1* ortholog in *E. grandiflorum*, *EgSTY1*, revealed strikingly similar expression patterns: concentrated expression in the carpel tips and petal nectaries (Fig. 5). In addition, dissection and RNAseq in *N. damascena* has revealed that *NdSTY1* is specifically expressed in petals, especially the region that contains the functional nectaries (R. Zhang & H. Z. Kong, pers. comm.). These results provide strong evidence to support a hypothesis that the novel role of *STY* genes controlling floral nectary development was acquired via co-option before the divergence of the sister families Berberidaceae and Ranunculaceae. It is worth noting that nectariferous petals are also common across other families of the Ranunculales (Erbar, 2014), and further studies will be required to examine whether this novel function is shared among this basal eudicot order.

On one hand, this conserved pattern is not surprising. Nectariferous petals are found across the Ranunculales, and we already have evidence suggesting that there is a commonly inherited petal identity program across these taxa (Sharma *et al.*, 2011). Therefore, it is plausible that this nectary determination program was commonly inherited with the petal program during the diversification of the order. On the other hand, it is still unclear as to how the novel expression domain of the *Aquilegia STY* genes was generated from a regulatory standpoint, and how they acquired their function in controlling nectary development. As mentioned earlier, we did find conserved regulatory elements associated with the *Aquilegia STY* homologs, but these motifs are most likely responsible for the conserved expression at the distal tips of lateral organs, rather than the novel domain associated with nectary development.

Combining our current knowledge of the genetic basis of floral nectary development, it is rather striking that two groups of genes, the *CRC* and *STY* homologs, both serve deeply conserved, but parallel, roles in building angiosperm carpels and have been independently recruited to control nectary development. Further studies will be required in order to determine how many genetic programs there actually are across the angiosperms for promoting development of the nectary, a feature that is considered to have arisen independently numerous times. One hypothesis regarding the co-option of *CRC* holds that this is related to the fact that floral nectaries are commonly associated with reproductive organs among the core eudicots (Lee, 2005), but this is clearly not the case with petal-associated nectaries in Ranunculales. It will be important to identify the upstream and downstream elements of both the *CRC* and *STY* homologs in regard to their functions in determining nectaries. We might predict that the downstream aspects of the pathway converge on common developmental programs related to secretion and sugar synthesis, but the regulatory wiring upstream of these pathways likely differ. Since the identification of *CRC* in 1999 (Bowman & Smyth, 1999), the *STY* homologs of the Ranunculales are the only alternative loci for the control of nectary development in flowering plants, providing a critical data point in understanding the evolutionary origin and developmental basis of nectaries, an important convergent trait.

Acknowledgements

The authors would like to thank members of the Kramer lab and two anonymous reviewers for very helpful comments on the manuscript. The authors would also like to thank Dr Bharti Sharma, who fixed and embedded the *Epimedium* material. This work was supported by NSF award IOS-1456217 to E.M.K.

Author contributions

The study was conceived of and designed by Y.M. and E.M.K. All experiments and data collection were conducted by Y.M. and J.I.B., with training and oversight provided by E.M.K. The manuscript was written and figures prepared by Y.M. with revisions by E.M.K.

ORCID

Elena M. Kramer http://orcid.org/0000-0002-5757-1088

References

Aloni R, Aloni E, Langhans M, Ullrich CI. 2006. Role of auxin in regulating Arabidopsis flower development. *Planta* **223**: 315–328.

Antoń S, Kamińska M. 2015. Comparative floral spur anatomy and nectar secretion in four representatives of Ranunculaceae. *Protoplasma* **252**: 1587–1601.

Baylis T, Cierlik I, Sundberg E, Mattsson J. 2013. *SHORT INTERNODES/STYLISH* genes, regulators of auxin biosynthesis, are involved in leaf vein development in *Arabidopsis thaliana*. *New Phytologist* **197**: 737–750.

Bender RL, Fekete ML, Klinkenberg PM, Hampton M, Bauer B, Malecha M, Lindgren K, Maki JA, Perera MADN, Nikolau BJ *et al.* 2013. PIN6 is required for nectary auxin response and short stamen development. *Plant Journal* **74**: 893–904.

Bernardello G. 2007. A systematic survey of floral nectaries. In: Nicolson SW, Massimo N, Ettore P, eds. *Nectaries and nectar*. Dordrecht, the Netherlands: Springer, 19–128.

Bowman JL, Smyth DR. 1999. *CRABS CLAW*, a gene that regulates carpel and nectary development in Arabidopsis, encodes a novel protein with zinc finger and helix-loop-helix domains. *Development* **126**: 2387–2396.

Brown WH. 1938. The bearing of nectaries on the phylogeny of flowering plants. *Proceedings of the American Philosophical Society* **79**: 549–595.

De La Barrera E, Nobel PS. 2004. Nectar: properties, floral aspects, and speculations on origin. *Trends in Plant Science* **9**: 65–69.

Eklund DM, Cierlik I, Staldal V, Claes AR, Vestman D, Chandler J, Sundberg E. 2011. Expression of Arabidopsis *SHORT INTERNODES/STYLISH* family genes in auxin biosynthesis zones of aerial organs is dependent on a GCC box-like regulatory element. *Plant Physiology* **157**: 2069–2080.

Eklund DM, Staldal V, Valsecchi I, Cierlik I, Eriksson C, Hiratsu K, Ohme-Takagi M, Sundstrom JF, Thelander M, Ezcurra I *et al.* 2010a. The *Arabidopsis thaliana* STYLISH1 protein acts as a transcriptional activator regulating auxin biosynthesis. *Plant Cell* **22**: 349–363.

Eklund DM, Thelander M, Landberg K, Staldal V, Nilsson A, Johansson M, Valsecchi I, Pederson ERA, Kowalczyk M, Ljung K *et al.* 2010b. Homologues of the *Arabidopsis thaliana SHI/STY/LRP1* genes control auxin biosynthesis and affect growth and development in the moss *Physcomitrella patens. Development* **137**: 1275–1284.

Endress PK. 1995. Floral structure and evolution in Ranunculanae. *Plant Systematics and Evolution* **9**: 47–61.

Erbar C. 2014. Nectar secretion and nectaries in basal angiosperms, magnoliids and non-core eudicots and a comparison with core eudicots. *Plant Diversity and Evolution* **131**: 63–143.

Filiault D, Ballerini E, Mandakova T, Akoz G, Derieg N, Schmutz J, Jenkins J, Grimwood J, Shu S, Hayes R *et al.* 2018. The *Aquilegia* genome: adaptive radiation and an extraordinarily polymorphic chromosome with a unique history. *bioRxiv* **5**: 264101.

Fourquin C, Vinauger-Douard M, Chambrier P, Berne-Dedieu A, Scutt CP. 2007. Functional conservation between *CRABS CLAW* orthologues from widely diverged angiosperms. *Annals of Botany* **100**: 651–657.

Gomariz-Fernández A, Sánchez-Gerschon V, Fourquin C, Ferrándiz C. 2017. The role of *SHI/STY/SRS* genes in organ growth and carpel development is conserved in the distant eudicot species *Arabidopsis thaliana* and *Nicotiana benthamiana. Frontiers in Plant Science* **8**: 1–17.

Gould B, Kramer EM. 2007. Virus-induced gene silencing as a tool for functional analyses in the emerging model plant *Aquilegia* (columbine, Ranunculaceae). *Plant Methods* **3**: 6.

Heil M. 2011. Nectar: generation, regulation and ecological functions. *Trends in Plant Science* **16**: 191–200.

Kramer EM. 2005. Methods for studying evolution of plant reproductive structures: comparative gene expression. *Methods in Enzymology* **395B**: 617–635.

Kuusk S, Sohlberg JJ, Long JA, Fridborg I, Sundberg E. 2002. *STY1* and *STY2* promote the formation of apical tissues during Arabidopsis gynoecium development. *Development* **4717**: 4707–4717.

Kuusk S, Sohlberg JJ, Magnus Eklund D, Sundberg E. 2006. Functionally redundant *SHI* family genes regulate Arabidopsis gynoecium development in a dose-dependent manner. *Plant Journal* **47**: 99–111.

Landberg K, Pederson ERA, Viaene T, Bozorg B, Friml J, Jonsson H, Thelander M, Sundberg E. 2013. The moss *Physcomitrella patens* reproductive organ development is highly organized, affected by the two *SHI/STY* genes and by the level of active auxin in the *SHI/STY* rxpression domain. *Plant Physiology* **162**: 1406–1419.

Larkin MA, Blackshields G, Brown NP, Chenna R, Mcgettigan PA, McWilliam H, Valentin F, Wallace IM, Wilm A, Lopez R *et al.* 2007. Clustal W and Clustal X version 2.0. *Bioinformatics* **23**: 2947–2948.

Lee J-Y. 2005. Recruitment of *CRABS CLAW* to promote nectary development within the eudicot clade. *Development* **132**: 5021–5032.

Livak KJ, Schmittgen TD. 2001. Analysis of relative gene expression data using real-time quantitative PCR and the 2(-Delta Delta C(T)) Method. *Methods* **25**: 402–408.

Marcos D, Berleth T. 2009. Visualizing auxin transport routes in Arabidopsis leaf primordia. *Methods in Molecular Biology* **495**: 11–21.

Matile P. 1956. Über den Stoffwechsel und die Auxinabhängigkeit der Nektarsekretion (On the metabolism and the auxin dependence of nectar secretion). *Berichte der Schweizerischen Botanischen Gesellschaft* **66**: 237–266.

Neiland MRM, Wilcock CC. 1998. Fruit set, nectar reward, and rarity in the Orchidaceae. *American Journal of Botany* **85**: 1657–1671.

Pacini E, Nepi M, Vesprini JL. 2003. Nectar biodiversity: a short review. *Plant Systematics and Evolution* **238**: 7–21.

Rasmussen DA, Kramer EM, Zimmer EA. 2009. One size fits all? Molecular evidence for a commonly inherited petal identity program in Ranunculales. *American Journal of Botany* **96**: 96–109.

Ruzin SE. 1999. *Plant microtechnique and microscopy.* New York, NY: Oxford University Press.

Sharma B, Guo C, Kong H, Kramer EM. 2011. Petal-specific subfunctionalization of an *APETALA3* paralog in the Ranunculales and its implications for petal evolution. *New Phytologist* **191**: 870–883.

Sharma B, Kramer E. 2012. Sub- and neo-functionalization of *APETALA3* paralogs have contributed to the evolution of novel floral organ identity in *Aquilegia* (columbine, Ranunculaceae). *New Phytologist* **197**: 949–957.

Shuel RW. 1964. Nectar secretion in excised flowers. III. The dual effect of indole-3-acetic acid. *Journal of Agricultural Research* **3**: 99–111.

Shuel RW. 1978. Nectar secretion in excised flowers. V. Effects of indoleacetic acid and sugar supply on distribution of [^{14}C]-sucrose in flower tissues and nectar. *Canadian Journal of Botany* **56**: 565–571.

Sohlberg JJ, Myrenås M, Kuusk S, Lagercrantz U, Kowalczyk M, Sandberg G, Sundberg E. 2006. *STY1* regulates auxin homeostasis and affects apical-basal patterning of the Arabidopsis gynoecium. *Plant Journal* **47**: 112–123.

Ståldal V, Cierlik I, Landberg K, Myrenås M, Sundström JF, Eklund DM, Chen S, Baylis T, Ljung K, Sundberg E. 2012. The *Arabidopsis thaliana* transcriptional activator *STYLISH1* regulates genes affecting stamen development, cell expansion and timing of flowering. *Plant Molecular Biology* **78**: 545–559.

Stamatakis A, Hoover P, Rougemont J. 2008. A rapid bootstrap algorithm for the RAxML web servers. *Systematic Biology* **57**: 758–771.

Stieger PA, Reinhardt D, Kuhlemeier C. 2002. The auxin influx carrier is essential for correct leaf positioning. *Plant Journal* **32**: 509–517.

Topp SH, Rasmussen SK. 2012. Evaluating the potential of *SHI* expression as a compacting tool for ornamental plants. *Plant Science* **187**: 19–30.

Wang W, Lu AM, Ren Y, Endress ME, Chen ZD. 2009. Phylogeny and classification of Ranunculales: evidence from four molecular loci and morphological data. *Perspectives in Plant Ecology, Evolution and Systematics* **11**: 81–110.

Whittall JB, Hodges SA. 2007. Pollinator shifts drive increasingly long nectar spurs in columbine flowers. *Nature* **447**: 706–709.

Yant L, Collani S, Puzey J, Levy C, Kramer EM, Kramer EM. 2015. Molecular basis for three-dimensional elaboration of the *Aquilegia* petal spur. *Proceedings of the Royal Society* **282**: 20 142 778.

Supporting Information

Additional supporting information may be found online in the Supporting Information section at the end of the article.

Fig. S1 Identification of the candidate genes.

Fig. S2 Expression patterns of *AqSTY2* and *AqLRP* during *A. coerulea* flower development.

Fig. S3 Quantitative RT-PCR showing the expression levels of *AqSTY1*, *AqSTY2* and *AqLRP* in WT *A. coerulea* tissues.

Fig. S4 Quantitative RT-PCR showing the silencing of *AqSTY1*, *AqSTY2* and *AqLRP* in both *AqSTY*-VIGS experiments.

Fig. S5 Relative nectar volume in WT *A. coerulea* flowers.

Fig. S6 Degenerate primer design to amplify putative *STY* homologs in various ranunculid taxa.

Fig. S7 Maximum likelihood phylogenetic tree showing the relationships between *STY* homologs amplified from 11 taxa from the Ranunculales.

Table S1 List of primers

Table S2 Stages of *Aquilegia* floral development

Please note: Wiley Blackwell are not responsible for the content or functionality of any Supporting Information supplied by the authors. Any queries (other than missing material) should be directed to the *New Phytologist* Central Office.